Hydrogen bonding versus π-interactions: their key competition in sildenafil solvates†

Rafael Barbas,[a] Rafel Prohens, *[a] Mercè Font-Bardia,[b]
Antonio Bauzá [c] and Antonio Frontera *[c]

†Laboratori de Química Farmacèutica (Unitat Associada al CSIC), Facultat de Farmàcia i Ciències de l'Alimentació, Institut de Biomedicina (IBUB), Universitat de Barcelona, Av. Joan XXIII 27−31, 08028 Barcelona, Spain
‡Departament de Cristal·lografia, Mineralogia i Dipòsits Minerals, Universitat de Barcelona, Martí Franquès s/n, 08028 Barcelona, Spain
§Unitat de Difracció de RX, Centres Científics i Tecnològics de la Universitat de Barcelona (CCiTUB), Solé i Sabarís 1−3, 08028 Barcelona, Spain
‖Departament de Nutrició, Ciències de l'Alimentaciói Gastronomia, Facultat de Farmàcia i Ciències de l'Alimentació, Universitat de Barcelona, Av. Prat de la Riba 171, 08921 Santa Coloma de Gramenet, Spain
⊥Institut de Biomedicina (IBUB) and Institut de Química Teòrica i Computacional (IQTCUB), Universitat de Barcelona, Av. Joan XXIII 27−31, 08028 Barcelona, Spain

Rafel Prohens: rafel@ccit.ub.edu
Antonio Frontera: toni.frontera@uib.es

Herein we report the X-ray characterization of four sildenafil solvates where the conformation of the pyrazoloij3,4-d]pyrimidine and phenyl rings depends on the solvent. It conditions the formation of an apparently innocent intramolecular H-bond that has a remarkable influence on the solid state architecture of the sildenafil solvates. DFT calculations indicate that a delicate balance between the energies of H-bonding and π–π (or lp–π) interactions are crucial.

A deep comprehension of weak interactions is essential to expand the field of supramolecular chemistry to new applications. For example, understanding the role of the solvent in the formation of crystals or co-crystals is a stimulating matter. Recently, it has been demonstrated that the formation of different types of co-crystals is related to the nature of the solvent, as it has been rationalized by comparing the strength of hydrogen and halogen bonding interactions.1 In this context, understanding the solid-state characteristics of drug substances is very important for the pharmaceutical industry. In particular, solvates of a drug substance can have significant consequences for storage, control or product performance.2

Sildenafil, 5-[2-ethoxy-5-(4-methylpiperazin-1-yl) sulfonylphenyl]-1-methyl-3-propyl-6H-pyrazoloij4,3-d]pyrimidin-7-one, improves penile erections in men with erectile dysfunction by selectively inhibiting the cGMP-specific phosphodiesterase type 5.3 The crystal structures of sildenafil citrate monohydrate and a sildenafil base have been reported.4,5 Moreover, sildenafil salts with saccharine6 and oxalic, fumaric, succinic and glutaric acids and co-crystals with adipic, pimelic, suberic and sebacic acids are also available.7 Furthermore, the cocrystals of sildenafil with acetylsalicylic acid and its salicylate salt have been recently characterized in an effort to combine an agent for preventing heart attacks and strokes with a drug that is contraindicated for men suffering from cardiovascular diseases.8

The study of the solid-state properties of solvates9 is of great importance since the presence of a solvent in the crystal gives them unique properties. For instance, the solubility and concomitant dissolution rate of a solvate are frequently different from those of the corresponding non-solvate affecting the bioavailability of the drug.10 In some cases, the solvent molecules are essential components of the packing, and in other cases, they simply occupy void spaces,11 and in this sense, we have recently shown that a new polymorph of sildenafil can be only obtained from the desolvation of an acetonitrile solvate.12 Since most of the drugs are administered as solid, the functioning of the final product can be modified. This obviously has a huge commercial impact at all stages of the active pharmaceutical ingredient development.

In this communication, we report four new solvates of sildenafil (Sil) (see Scheme 1) that consist of co-crystals of a Sil base with chloroform, toluene, anisole and dioxane.‡ We paid attention to the intramolecular H-bond that maintains the co-planarity of the pyrazoloij3,4-d]pyrimidine and phenyl rings (see Scheme 1a). We found that this H-bond is solvent dependent and its rupture has a strong influence in the crystal packing. Remarkably, there are 25 X-ray structures containing sildenafil in the CSD (salts and/or solvates) and all of them exhibit the intramolecular N–H···O H-bond between the

pyrimidine ring and the ethoxy substituent of the phenyl ring (see the full list of CSD codes in Table S1†). In 24 out of the 25 structures, the pyrazoloij3,4-d]pyrimidine and phenyl rings are coplanar, and in only one case, (hydrogen fumarate salt) the phenyl ring is slightly rotated (28°) with the N–H···O H-bond nevertheless present. Herein, for the first time, aromatic solvents (toluene and anisole) are used to generate solvates of sildenafil. Quite remarkably, these solvents are able to disrupt the intramolecular H-bonds facilitating the formation of self-assembled receptors (see Scheme 1a) which are capable of encapsulating the aromatic solvent due to the formation of electrostatically enhanced π-stacking interactions as evidenced by DFT calculations.

Partial crystal data details are given in Table 1 (see the ESI† for the complete crystal-data details). The X-ray structures of solvates 1 (sildenafil–chloroform) and 2 (sildenafil–toluene) are shown in Fig. 1 and that of 3 in Fig. S1† along with the rotational angles. In solvates 2 and 3, the toluene and anisole molecules lie disordered about the inversion centre. It can be observed that the pyrimidine and phenyl rings are coplanar in 1 and almost perpendicular in 2 (same behaviour in sildenafil–anisol 3 and sildenafil–dioxane 4, vide infra). Compounds 2, 3 and 4 are essentially isomorphous with very similar intermolecular N3–H3···N2* H-bonding (* = x, 3/2 − y, 1/2 + z), as further explained below. We have optimized the sildenafil base using the coplanar conformation and its rotamer (at 90°, see Fig. S2†) and the energetic difference is 5.0 kcal mol−1 which approximately counts for the strength of the intramolecular H-bond. The solid state architecture of compound 1 compared to that of the published form5 of sildenafil is shown in Fig. 2. In both compounds, the crystal packing is basically dominated by the formation of π-stacking interactions due to the large aromatic surface provided by the coplanarity of the pyrazoloij3,4-d]pyrimidine and phenyl rings. The presence of the chloroform molecule in the structure only changes the parallel arrangement of the π-stacked columns to a zigzag disposition. In sharp contrast to the solid state architectures observed for the published sildenafil-based structures and solvate 1, the toluene and anisole solvates exhibit a totally different structure. Self-assembly dimers are formed in the solid states of 2 and 3 that generate a cavity suitable for interacting with the aromatic solvent, as detailed in Fig. 3. The aromatic solvent is able to disrupt the otherwise ordered 3D architectures of 1 and non-solvated sildenafil since it provides the possibility to establish electrostatically enhanced π–π interactions that are able to compensate for the breakage of the intramolecular H-bond and the π-stacking interactions between the extended π-systems of sildenafil as highlighted in Fig. 2. In addition, the intramolecular NH···O bond is replaced by an intermolecular NH···N bond involving the N-atom of the piperazine ring as the H-bond acceptor in solvates 2–4 (see Fig. 4). Moreover, in Fig. 4, we have indicated the geometric features of the H-bond in the solvates and in the DFT optimized dimer. In the DFT-optimized H-bonded dimer, the distance is longer than that in the X-ray structures, likely due to the fact that the crystal packing effects are not reflected in the calculations. The interaction energy of the complex is ΔEHB = −6.3 kcal mol−1, slightly stronger than that of the intramolecular H-bond in line with the higher basicity of the tertiary amine group. This

intermolecular H-bond further contributed to the stabilization of solvates 2–4 complementing the π-stacking interactions shown in Fig. 3.

The variations in the electronic distribution of the molecular entities are the origin of attractive and repulsive electrostatic intermolecular forces. The solid state architecture of the compounds comes from a compromise between repulsive and attractive forces. In this sense, the geometry adopted by the different assemblies that can be found in X-ray structures tends to maximize the complementarity between the electron rich and electron poor regions of two or more molecules. In order to determine the electron rich and poor regions of sildenafil, we have computed the molecular electrostatic potential (MEP) values and plotted them onto the van der Waals surface (see Fig. 5). The most negative region is located on the sulfoxide group and the most positive one on the H-atoms of the ethoxy substituent. Moreover, the H-atoms of the methyl substituent of the pyrazolo ring are also positive (+17 kcal mol−1). An interesting feature is that the pyrimidine ring exhibits a positive MEP value over the center of the ring. Even more remarkably, if the MEP surface is computed for the 90° rotated conformation (see ESI,† Fig. S3), the MEP value at the pyrimidine ring increases from 5 to 8 kcal mol−1, thus enhancing the π-acidity of the ring. Therefore, the formation of π–π stacking interactions with electron rich aromatic rings is favored. This likely explains the formation of the assemblies shown in Fig. 3 when electron rich aromatic solvents like anisole and toluene are involved. We have computed the interaction energies of the cage with the aromatic solvents, which are $\Delta E1 = -14.4$ kcal mol−1 for toluene and $\Delta E2 = -12.6$ kcal mol−1 for anisole. These large interaction energies are due to the formation of two enhanced π–π stacking interactions and additional van der Waals interactions with the other groups of the cavity (vide infra). The formation energy of the cage itself (two C–H···O H-bonds) is −6.0 kcal mol−1, which is not able to compensate for the destabilization energy due to the disruption of two intramolecular H-bonds. However, this is largely compensated by the host–guest interaction.

Encouraged by these results, we envisaged the utilization of electron rich solvents (lone pair donors) and investigate if they are also able to provoke the formation of supramolecular cages instead of the 2D layers shown in Fig. 2. Gratifyingly, we succeeded in the co-crystallization of sildenafil with dioxane (see Fig. 6), and it can be observed that one lone pair of the O atom of dioxane is pointing to the π-system of the pyrimidine ring, in good agreement with the MEP analysis. Moreover, the other lone pair establishes a C–H···O interaction with one aromatic H-atom. Due to the chair conformation of the guest, the H-bonds that govern the formation of the self-assembled receptor are longer in 4 compared to those in 2 or 3 where the guest is a planar aromatic ring. Therefore, the cage is flexible enough to accommodate the guest inside the cavity.

Finally, we have also performed an NCI plot index analysis to characterize the non-covalent interactions between the selfassembled cage and either toluene (as example of an aromatic guest) or dioxane. The NCI plot is a convenient visualization index because it easily enables the visualization and identification of non-covalent interactions efficiently.13 It is based on the peaks that appear in the reduced density gradient (RDG) at low densities (see ref. 14 for a more comprehensive treatment). When a

supramolecular complex is formed, there is a crucial change in the RDG at the critical points in between molecules due to the annihilation of the density gradient at these points. Therefore, the NCI analysis allows an assessment of host–guest complementarity and the extent to which weak interactions stabilize a complex. The information provided is essentially qualitative, that is, which molecular regions interact. The color scheme is a red-yellow-green-blue scale with red for ρ+ cut (repulsive) and blue for ρ −cut (attractive). The yellow and green surfaces correspond to weak repulsive and weak attractive interactions, respectively. The representations of the NCI plots computed for solvates 2 and 4 are shown in Fig. 7. In both solvates, a very small isosurface can be detected between the –NCH3 group and the O atom of the sulphoxide group, thus characterizing the H-bond that is responsible for the formation of the cage. In solvate 2, extended green regions are present between the aromatic ring of toluene and both pyrazoloij3,4-d]pyrimidine moieties, thus characterizing the π-stacking interactions. In solvate 4, the H-bond and lp–π interactions involving the O atoms of dioxane are clearly represented by small isosurfaces. In addition, a more extended isosurface is located between the H atoms of dioxane and the pyrazoloij3,4-d]pyrimidine moiety, thus revealing the existence of C–H···π interactions that further stabilize the assembly. Finally, in both complexes, additional green isosurfaces are located between the guest and the cage walls confirming the existence of weak interactions. These are more evident in solvate 2 compared to 4, in agreement with the stronger binding of toluene. This is likely due to the chair conformation of dioxane that causes the formation of a larger cavity and consequently the vdW contacts of the guest are less important.

In conclusion, we have reported the X-ray structure of several sildenafil solvates. The utilization of aromatic solvates causes a significant change in the conformation of the sildenafil moiety. The otherwise planar π-system composed of the phenyl and pyrazoloij3,4-d]pyrimidine rings changes to an almost perpendicular arrangement of the rings and the intramolecular H-bond is disrupted. All sildenafil solvates and salts reported so far present a co-planar disposition of both π-systems. Therefore, complexes 2–4 are the first examples of sildenafil X-ray structures exhibiting the formation of selfassembled dimers in the solid state, which are adequate for trapping aromatic solvent molecules and dioxane. Therefore, the results reported herein might be used to develop a new line of research devoted to the co-crystallization of sildenafil with biologically relevant planar molecules like aromatic amino-acids or nucleobases which may have enhanced pharmaceutical properties.

Financial support from the MINECO of Spain (projects CTQ2014-57393-C2-1-P and CTQ2017-85821-R FEDER funds) is gratefully acknowledged.

1 C. C. Robertson, J. S. Wright, E. J. Carrington, R. N. Perutz, C. A. Hunter and L. Brammer, Chem. Sci., 2017, 8, 5392.

2 Applied Biopharmaceutics & Pharmacokinetics, ed. L. Shargel and A. B. C. Yu, Mc Graw-Hill, New York, 7th edn, 2016.

3 (a) A. Laties and E. Zrenner, Prog. Retinal Eye Res., 2002, 21, 485–506; (b) X.-D. Zhuang, M. Long, F. Li, X. Hu, X.-X. Liao and Z.-M. Du, Int. J. Cardiol., 2014, 172, 581.

4 H. S. Yathirajan, B. Nagaraj, P. Nagaraja and M. Bolte, Acta Crystallogr., Sect. E: Struct. Rep. Online, 2005, 61, o489.

5 D. Stepanovs and A. Mishnev, Z. Naturforsch., B: J. Chem. Sci., 2012, 67, 491.

6 R. Banerjee, P. M. Bhatt and G. R. Desiraju, Cryst. Growth Des., 2006, 6, 1468.

7 P. Sanphui, S. Tothadi, S. Ganguly and G. R. Desiraju, Mol. Pharmaceutics, 2013, 10, 4687.

8 (a) M. Žegarac, E. Lekšic, P. Šket, J. Plavec, M. D. Bogdanovic, D.-K. Bucar, M. Dumic and E. Meštrovic, CrystEngComm, 2014, 16, 32; (b) D. Stepanovs, M. Jureb and A. Mishnev, Mendeleev Commun., 2015, 25, 49–50.

9 (a) S. R. Byrn, G. Zografi and X. Chen, Solid-State Properties of Pharmaceutical Materials, Chapter 3: Solvates and Hydrates, John Wiley & Sons, Inc., 1st edn, 2017; (b) B. Rodríguez-Spong, C. P. Price, A. Jayasankar, A. J. Matzger and N. Rodríguez-Hornedo, Adv. Drug Delivery Rev., 2004, 56, 241–274; (c) U. J. Griesser, The Importance of Solvates, in Polymorphism in the Pharmaceutical Industry, ed. R. Hilfiker, Wiley-VCH Verlag GmbH & Co. Weinheim, Germany, 2006.

10 (a) S. R. Byrn, R. R. Pfeiffer and J. G. Stowell, Solid-State Chemistry of Drugs, SSCI Inc., West Lafayette, IN, 2nd edn, 1999; (b) S. L. Morissette, O. Almarsson, M. L. Peterson, J. F. Remenar, M. J. Read, A. V. Lemmo, S. Ellis, M. J. Cima and C. R. Gardner, Adv. Drug Delivery Rev., 2004, 56, 275.

11 V. S. S. Kumar, F. C. Pigge and N. P. Rath, Cryst. Growth Des., 2004, 4, 651.

12 R. Barbas, M. Font-Bardia and R. Prohens, Cryst. Growth Des., 2018, 18, DOI: 10.1021/acs.cgd.8b00683.

13 J. Contreras-García, E. R. Johnson, S. Keinan, R. Chaudret J.-P. Piquemal, D. N. Beratan and W. Yang, J. Chem. Theory Comput., 2011, 7, 625–632.

14 E. R. Johnson, S. Keinan, P. Mori-Sanchez, J. Contreras-Garcia, A. J. Cohen and W. Yang, J. Am. Chem. Soc., 2010, 132, 6498–6506.

Legends to figures

Scheme 1 (a) Structure of compounds 1–4. (b) Self-assembled dimer.

Figure. 1 X-ray structure of compounds 1 (a) and 2 (b) with the rotational angles indicated.

Figure.2. Crystal packing of QEGTUT (a) and solvate 1 (b).

Figure.3 Self-assembled dimers observed in the solid states of solvates 2 (a) and 3 (b). The binding energies of the aromatic guest with the supramolecular receptor are also given. Distances are in Å. H-Atoms are omitted for clarity apart from those that belong to the methyl groups. The guest is represented as a space-filling model with 70% transparency**.**

Figure.4. Optimized dimer of sildenafil and some geometric features of the intermolecular H-bond observed in the solid states of solvates 2–4. Distances are in Å. H-Atoms are omitted for clarity apart from NH

Figure.5 Molecular electrostatic potential surface (isovalue 0.002 a.u.) map of sildenafil. The MEP values at selected points of the surface are given in kcal mol−1.

Figure.6 X-ray structure of solvate 4 with the lp–π interaction indicated. (a) Self-assembled dimer observed in the solid state of solvate 4 (b) and the binding energy with dioxane. Distances are in Å.

Figure.7 NCI plots of the self-assembled cages of solvates 2 (a) and 4 (b). The gradient cut-off is s = 0.35 au and the color scale is $-0.04 < \rho < 0.04$ au.

SCHEME 1

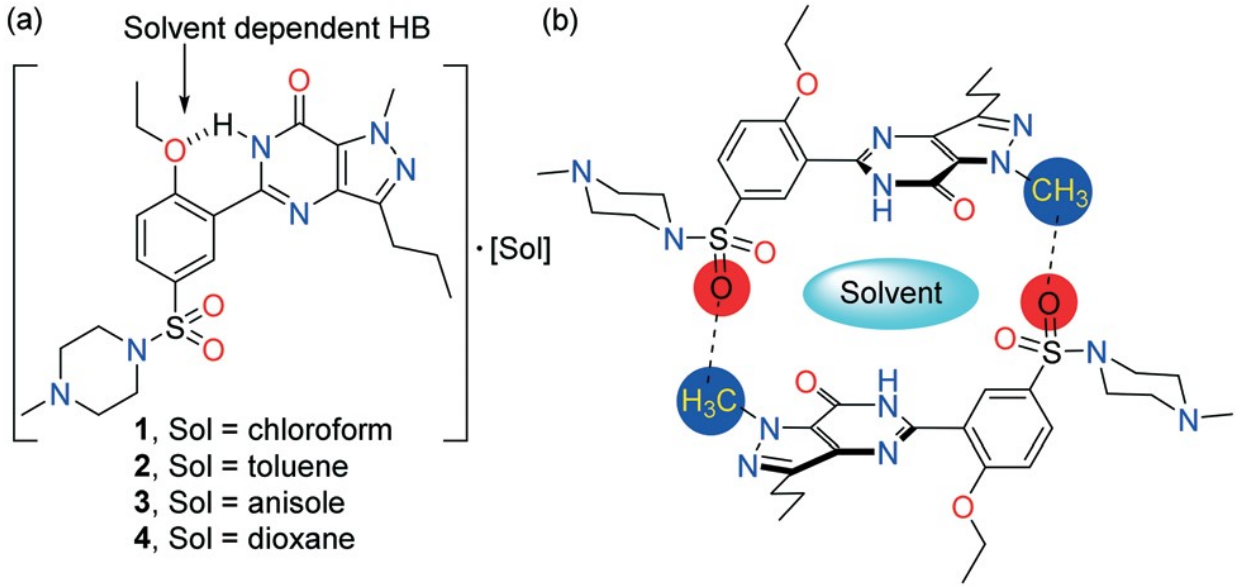
(a)
Solvent dependent HB
· [Sol]
1, Sol = chloroform
2, Sol = toluene
3, Sol = anisole
4, Sol = dioxane
(b)
Solvent
CH3
H3C

FIGURE 1

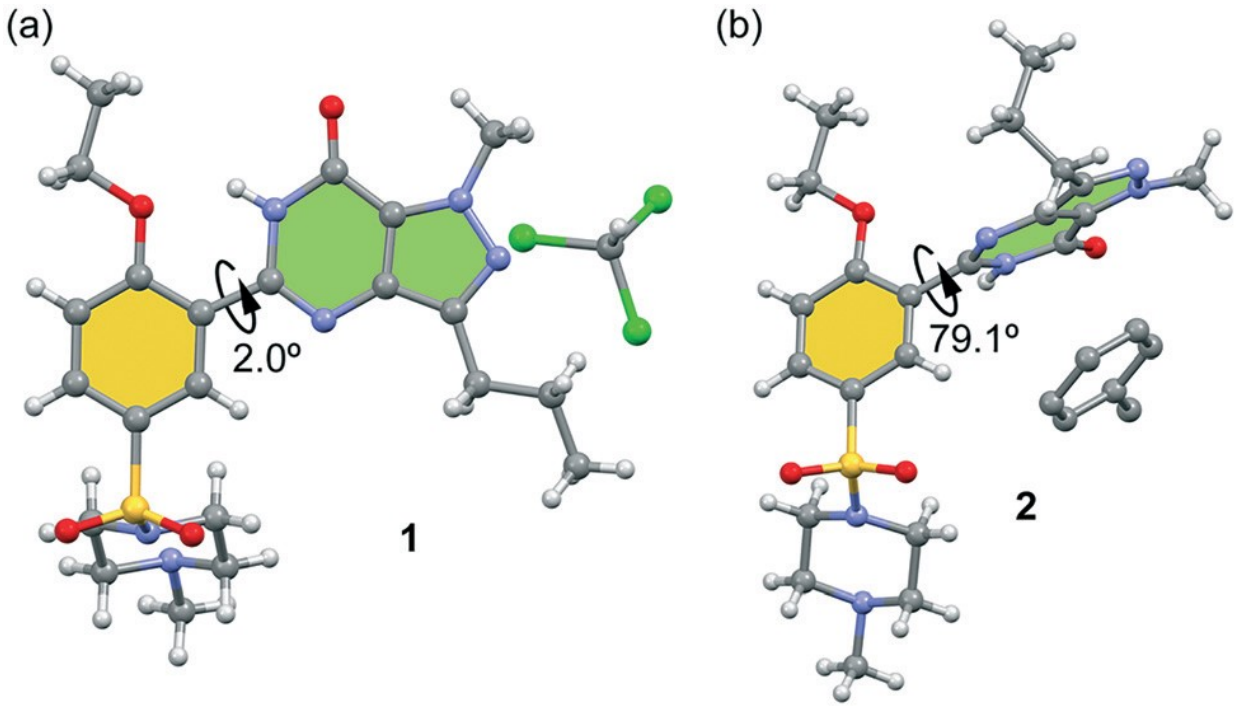

FIGURE 2

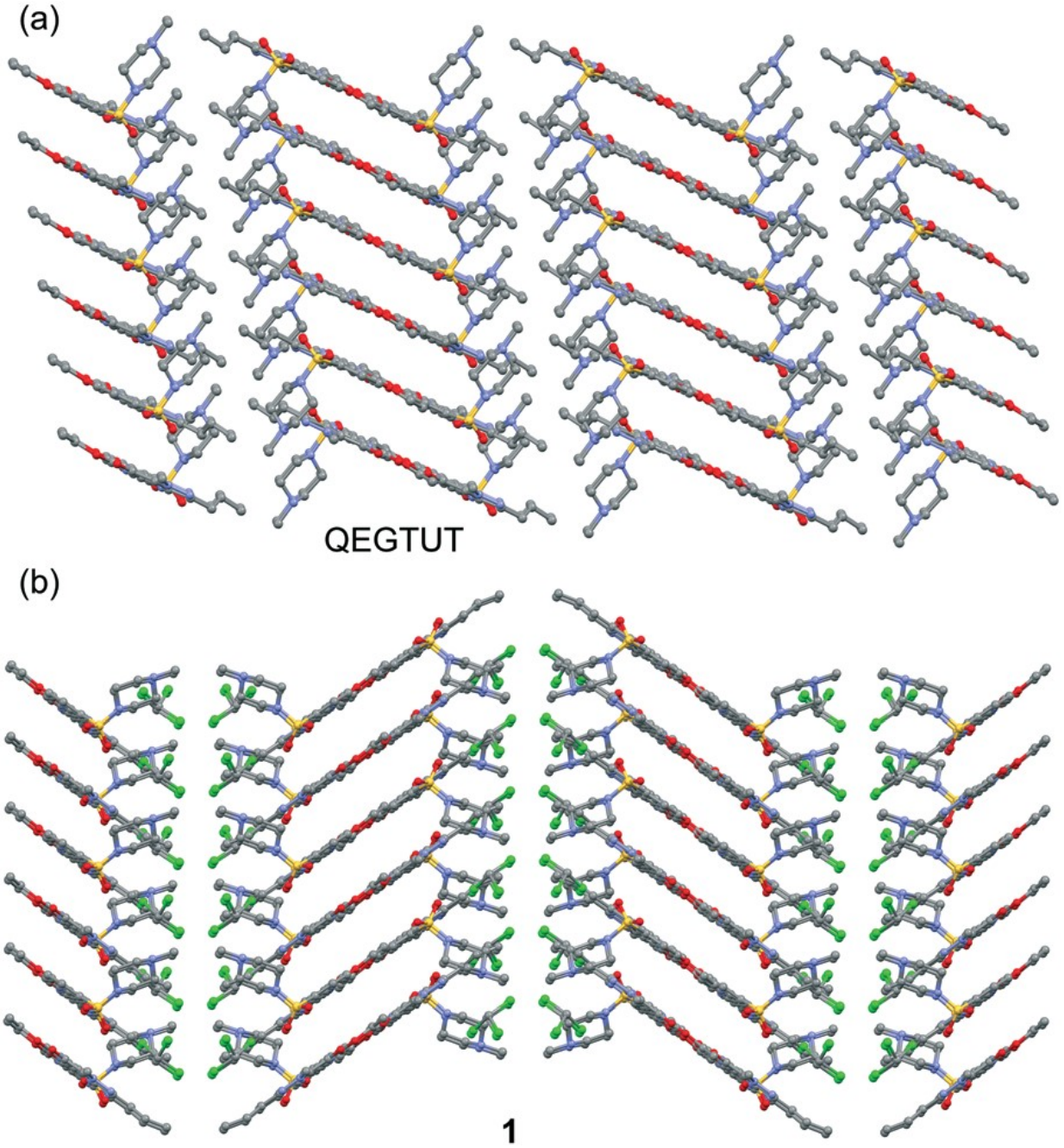

FIGURE 3

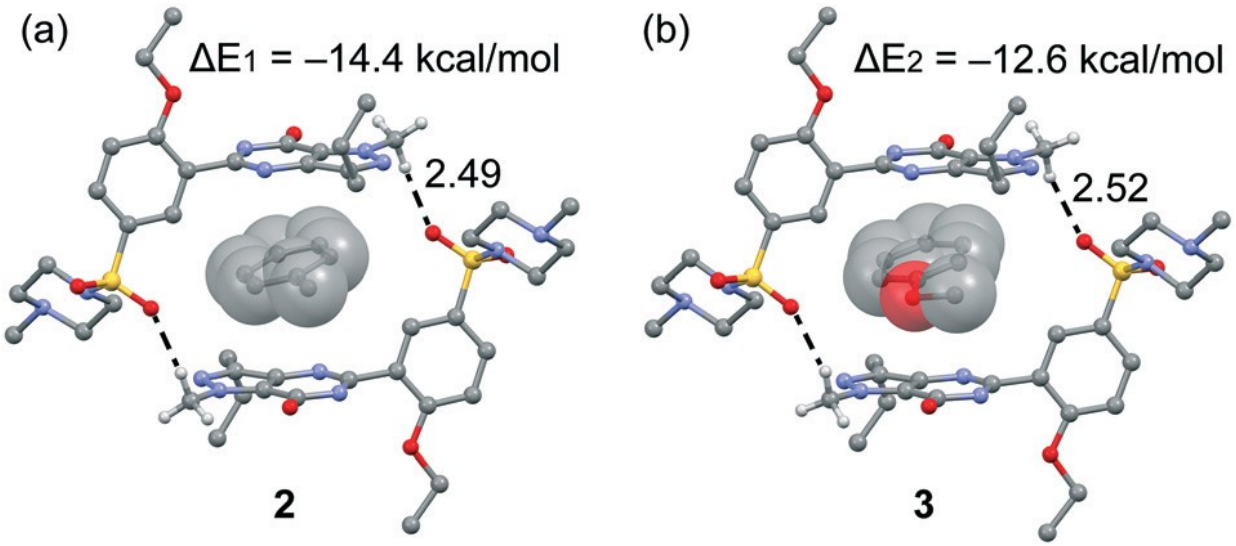

271 **FIGURE 4**

272

273

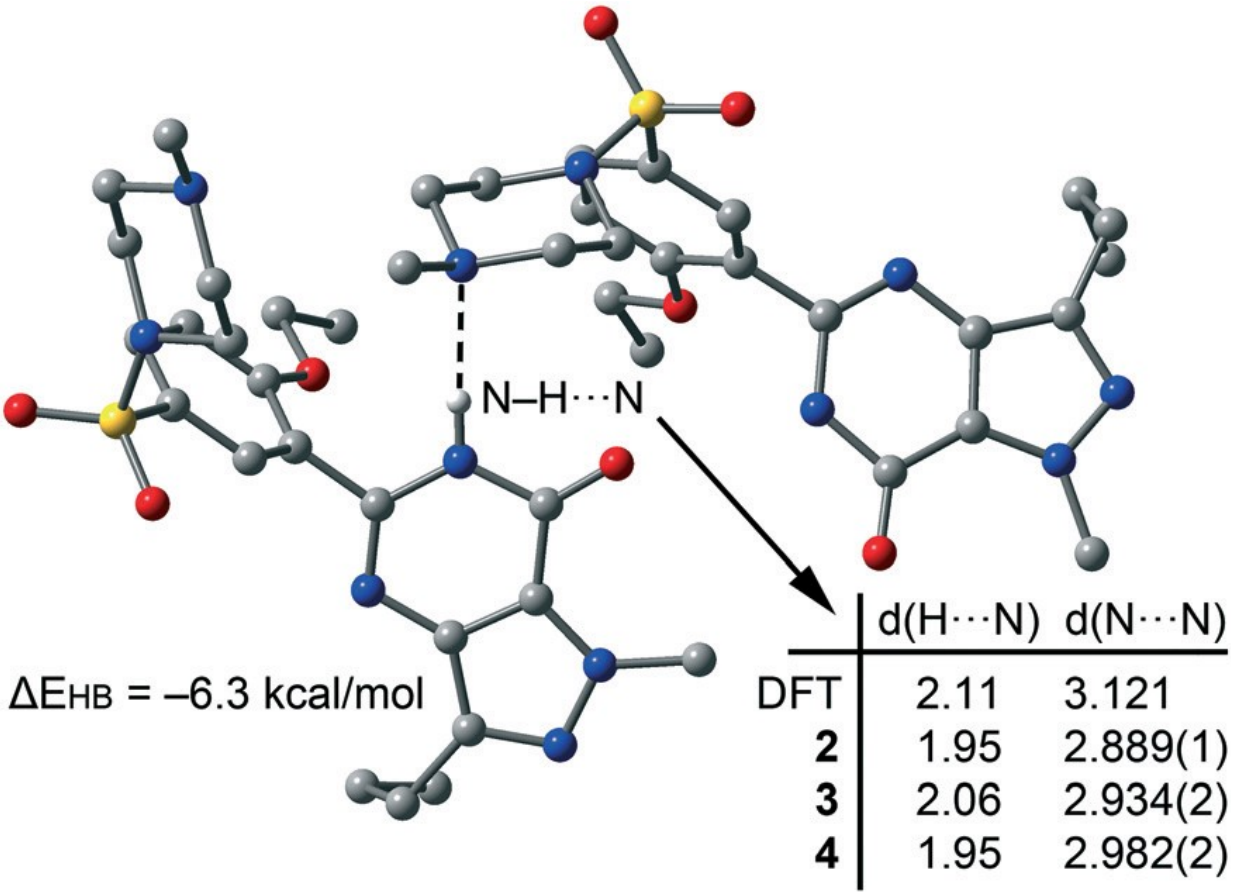

	d(H···N)	d(N···N)
DFT	2.11	3.121
2	1.95	2.889(1)
3	2.06	2.934(2)
4	1.95	2.982(2)

274

275

276 **FIGURE 5**

277

278

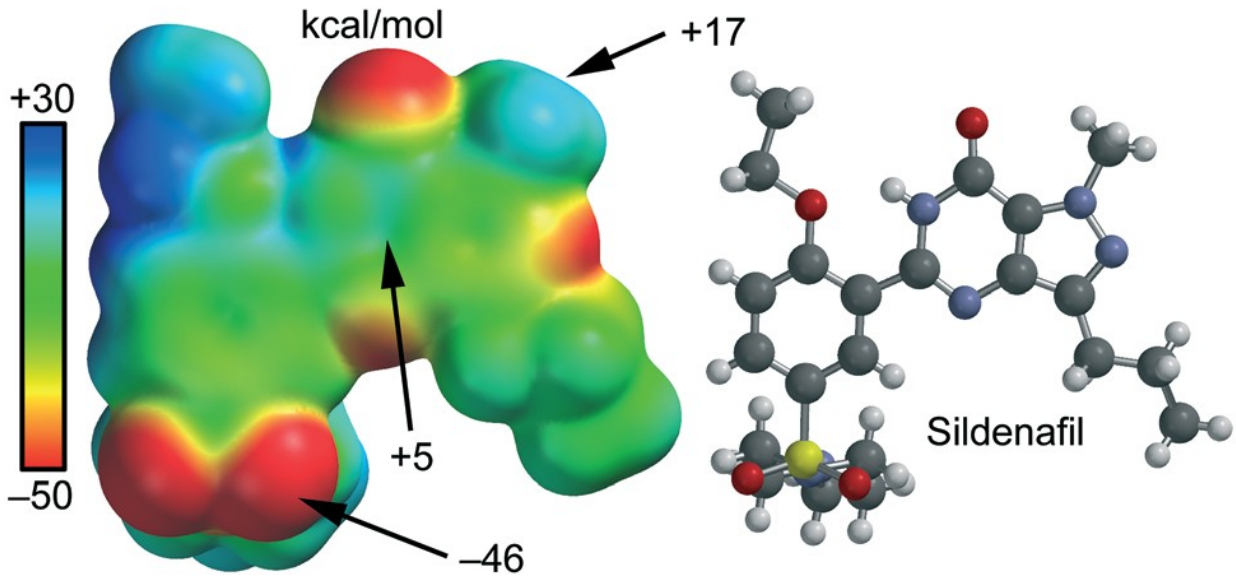

279

280

FIGURE 6

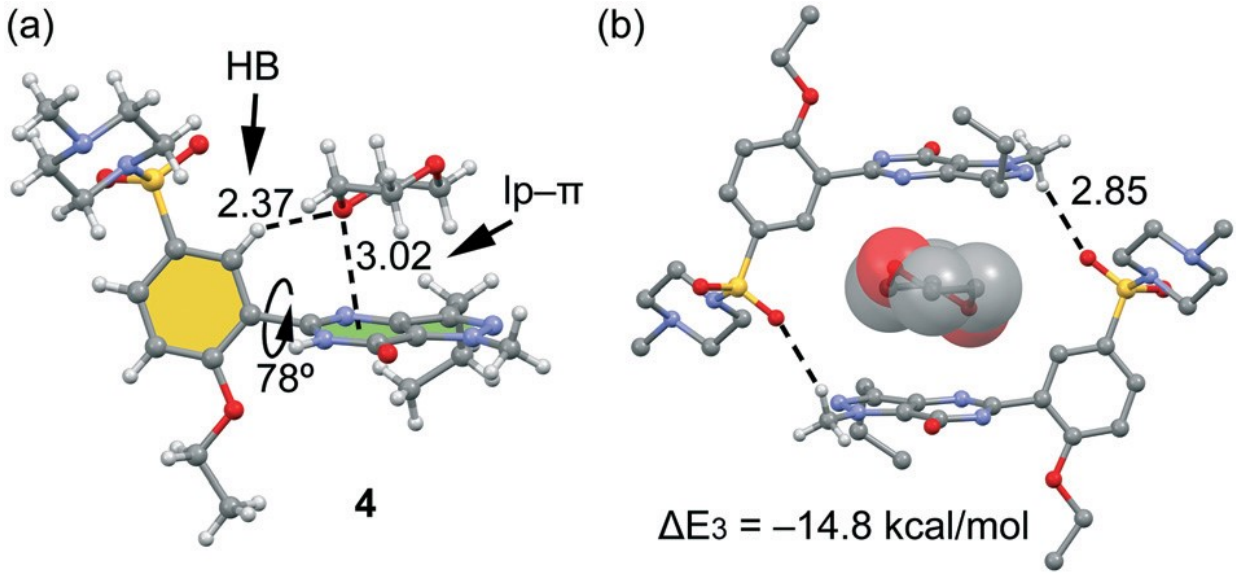

286 **FIGURE 7**

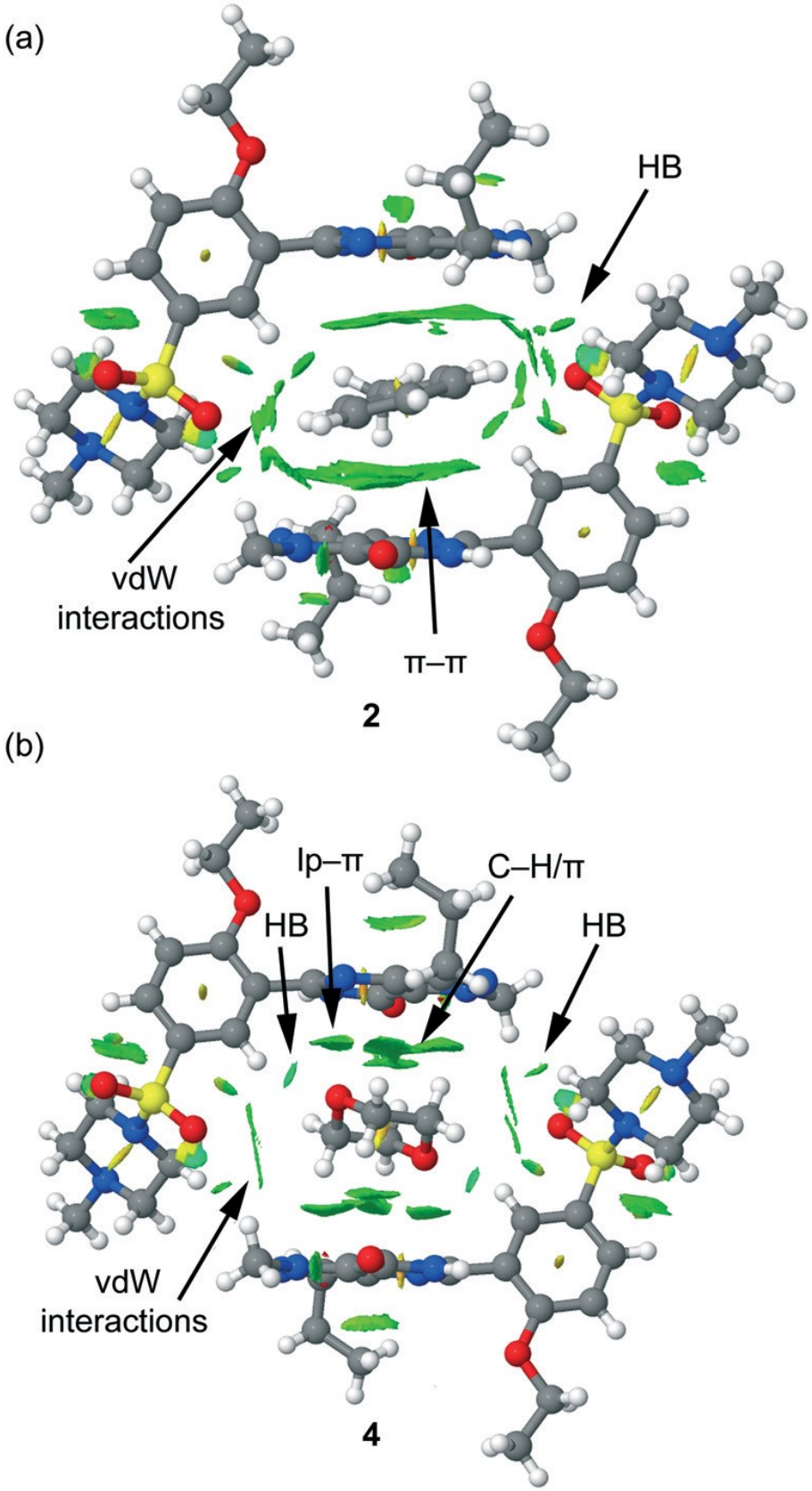

287

288

289 **Table 1** Crystallographic data and refinement details of solvates 1–4

290

Structure	1	2	3	4
Empirical formula	$C_{23}H_{31}Cl_3N_6O_6S$	$C_{51}H_{68}N_{12}O_8S_2$	$C_{51}H_{68}N_{12}O_8S_2$	$C_{24}H_{34}N_6O_2S$
Formula weight	593.95	1041.29	1057.29	518.63
Temperature (K)	301(2)	100(2)	100(2)	100(2)
Wavelength (Å)	0.71073	0.71073	0.71073	0.71073
Crystal system	Orthorhombic	Monoclinic	Monoclinic	Monoclinic
Space group	*Pbca*	$P2_1/c$	$P2_1/c$	$P2_1/c$
a, *b*, *c* (Å)	16.3399(7), 8.5767(3), 40.1148(16)	14.8287(6), 14.3781(6), 12.7277(5)	14.8822(7), 14.2697(7), 12.842(6)	15.6055(5), 13.5523(4), 12.5064(4)
α, β, γ (°)	90, 90, 90	90, 106.4830(10), 90	90.0, 106.409(2), 90.0	90, 106.3620(10), 90
Volume (Å^3)	5621.8(4)	2602.13(18)	2610.4(2)	2537.86(14)
Z, δ (calc.) Mg m^{-3}	8, 1.403	2, 1.329	2, 1.345	4, 1.357
CCDC	1832572	1821374	1821371	1832573

291